Available online at www.sciencedirect.com
ScienceDirect
Catalysis Today 127 (2007) 295–303
CATALYSIS TODAY
www.elsevier.com/locate/cattod

Methanol reformate treatment in a PEM fuel cell-reactor

F.M. Sapountzi, M.N. Tsampas, C.G. Vayenas *

Department of Chemical Engineering, University of Patras, GR-26504 Patras, Greece

Available online 2 May 2007

Abstract

The treatment of methanol reformate, containing up to 2500 ppm CO, by the anode of a PEM fuel cell, operating as a preferential oxidation (PROX) reactor, was investigated in order to examine the possibility of electrochemically promoting the water–gas-shift (WGS) reaction and thus making the gas mixture suitable for anodic oxidation. It was found that the electrochemical promotion effect plays a significant role in a normal fuel cell operation (air at the cathode) but not in a hydrogen pumping operation (H_2 at the cathode). This implies that the role of oxygen crossover in the electropromotion (EP) of the WGS reaction and in the CO oxidation is vital. During fuel cell operation, the increase in the rate of CO consumption over a Pt/C anode is 2.5 times larger than the electrochemical rate, $I/2F$ of CO consumption, while for oxygen bleeding conditions (fuel mixture + 1% O_2 at the anode) the increase is up to five times larger than $I/2F$, i.e. the Faradaic efficiency is up to 5. This shows that the catalytic properties of the Pt anode are significantly modified by varying catalyst potential and by the extent of O_2 crossover.

The effect of temperature, gas composition, membrane thickness and Pt anode alloying with Cu was studied. It was found that the rate of CO consumption is significantly enhanced by increasing T, p_{H_2} and increasing O_2 crossover rate. Also the Faradaic efficiency reaches even higher values (up to 9) when using PtCu/C anodes. However, the Faradaic efficiency drops in general below 100% at high current densities and CO conversion levels.

© 2007 Elsevier B.V. All rights reserved.

Keywords: Electrochemical promotion of catalysis (EPOC); NEMCA effect; PEM fuel cell; CO-poisoning; Oxygen crossover; PROX

1. Introduction

PEM fuel cells have gained much scientific and technological interest in recent years due to their high performance when operating with hydrogen fuel. During hydrogen production from hydrocarbon or alcohol reforming, carbon monoxide is formed as well. Even after thorough treatment of the thus produced hydrogen, small traces of CO (in ppm levels) remain in the hydrogen stream which adsorb on the anode and lead to CO-poisoning, thus impairing significantly the cell performance [1,2].

A method used in previous studies to overcome this problem is to mix the gas feed with oxygen (oxygen bleeding) in order to achieve CO oxidation on the anode. However, this method involves complicated control systems in order to maintain safe fuel cell operation. Moreover, it has been documented in literature that only a small amount of oxygen participates in the oxidation of CO and the remaining oxygen could lead to a decline of the fuel cell performance because of its reaction with the fuel (H_2) [3–5]. Adding hydrogen peroxide to the fuel stream has also been tried as a method to minimize the CO contamination [6]. Another approach is to use a preferential oxidation (PROX) reactor before the fuel cell in order to convert CO into CO_2 via the water–gas-shift reaction or to use the fuel cell itself for this purpose [7].

The aim of this work was to study the electrochemical promotion effect of two different reactions taking place at the anode of a PEM fuel cell:

(1) CO oxidation due to either oxygen crossover through Nafion or oxygen bleeding and
(2) the water–gas-shift reaction when the cell operates as a PROX reactor.

A state-of-the-art PEM fuel cell [8–11] was used in our study, where the NEMCA behavior of the above reactions was examined on Pt and PtCu catalysts on Nafion membranes (Nafion 117 and 1135). The cell was run under extreme

* Corresponding author.
E-mail address: cat@chemeng.upatras.gr (C.G. Vayenas).

0920-5861/$ – see front matter © 2007 Elsevier B.V. All rights reserved.
doi:10.1016/j.cattod.2007.03.016

CO-poisoning conditions, using at the anode a gas mixture simulating an untreated methanol reformate gas, thus the currents obtained were typically lower than 100 mA.

The electrochemical promotion of catalysis, which is also known in the literature as the NEMCA effect (Non-Faradaic Electrochemical Modification of Catalytic Activity) is a phenomenon where application of a small current or potential on a catalyst which is in contact with a solid electrolyte results to non-Faradaic changes on the catalytic activity and selectivity. In most cases, these changes are reversible, as they disappear when the current or potential application is interrupted. Electrochemical promotion allows for in situ control of catalyst activity and selectivity via application of a current or potential between the catalyst (working electrode, WE) and a conductive counter electrode (CE), as a result of controlled migration of promoting species from the electrolyte support to the metal/gas catalytic interface [12–16]. In this study, the anode and cathode of a PEM fuel cell play the role of the WE and CE, respectively.

Two parameters are commonly used to describe the magnitude of electrochemical promotion:

a. The Faradaic efficiency, Λ is defined from

$$\Lambda = \frac{\Delta r}{(I/2F)}, \quad (1)$$

where Δr is the change in the catalytic rate caused by the current or potential application, I the applied current and F is the Faraday's constant. When $|\Lambda| \geq 1$, the changes in the catalytic rate are non-Faradaic and the reaction exhibits NEMCA behavior, while pure electrocatalysis dominates when $|\Lambda| < 1$. A reaction is called electrophobic when $\Lambda > 1$, and electrophilic when $\Lambda < -1$ [12–17].

b. The rate enhancement ratio, ρ, is defined from

$$\rho = \frac{r}{r_o}, \quad (2)$$

where r is the electrochemically promoted catalytic rate and r_o is the unpromoted catalytic rate.

In a recent paper [18], we have presented some preliminary results on the electrochemical promotion of the PEM fuel cell-reactor operating on methanol reformate gas. That study was limited to low temperatures (30 °C) and low H_2 partial pressures. Here we present new results obtained at operating temperatures up to 80 °C, higher (up to 90%) hydrogen partial pressures and also using PtCu/C anode catalysts.

2. Experimental

A PEM fuel cell provided by NuVant (Fig. 1) was used in the present work, similarly with previous studies [8–11]. Three different membrane electrode assemblies (MEAs) of anode/electrolyte/cathode were constructed; a Pt/Nafion 117/Pt, a Pt/Nafion 1135/Pt, and a PtCu/Nafion 117/Pt assembly. The Pt electrodes had metal loading of 0.5 mg Pt/cm^2 (unsupported Pt black) on E-TEK carbon cloth. Nafion 117 with nominal thickness of 185 μm and Nafion 1135 with nominal thickness

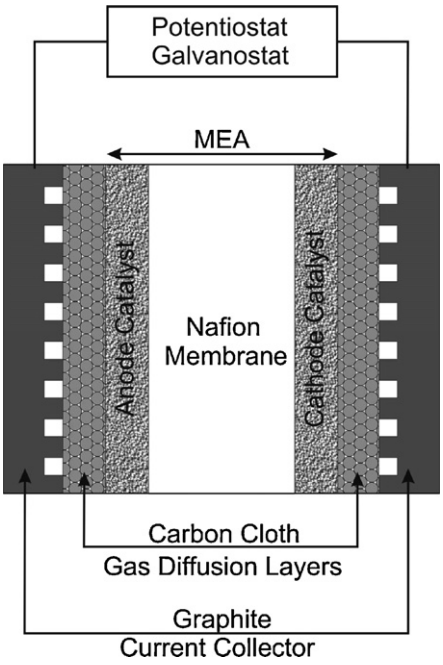

Fig. 1. Schematic of the PEMFC geometry [13–15] and basic electrical circuit showing the membrane electrode assembly (MEA) and the gas diffusion layers at the anode and cathode.

of 90 μm obtained from Dupont were used as the proton conductor. All the membranes were prepared under hot-pressing conditions (under 1 metric tonne, at 120 °C for 3 min). The electrode geometric surface area was in all cases 2.3 cm × 2.3 cm = 5.29 cm^2.

In the case of the PtCu/Nafion 117/Pt cell, the Pt electrode (cathode electrode) had a metal loading of 0.5 mg Pt/cm^2 (unsupported Pt black) on E-TEK carbon cloth and the anode was a 40% HP Pt:Cu alloy (1:1 a/o) on Vulcan XC-72 provided by E-TEK.

The cells were run under three different modes:

i. normal fuel cell operation (anode feed: fuel mixture–cathode feed: air),
ii. hydrogen pumping operation (anode feed: fuel mixture–cathode feed: H_2) and
iii. oxygen bleeding operation (anode feed: fuel mixture + O_2–cathode feed: air).

Both anode and cathode feeds were continuously humidified via thermostated gas saturators. For the fuel cell operation, a certified Messer-Griesheim dry gas mixture of 33.66% CO_2, 33.71% H_2, 0.63% CO and 31.98% N_2 was used at the anode and Air Liquide synthetic air was fed to the cathode. The same gas mixture was supplied to the anode during hydrogen pumping operation while Air Liquide certified 1% H_2 in He was fed to the cathode. For the oxygen bleeding mode an Air Liquide certified 1.2% O_2 in He mixture was supplied to the anode after mixing with the above Messer-Griesheim gas mixture, while Air Liquide synthetic air was fed to the cathode. When required, the gases were diluted by Messer-Griesheim He or by Messer-Griesheim H_2. We diluted the anode fuel mixture

with Messer-Griesheim He, in order to have several different gas compositions. We have labeled them according to their CO content as "700 ppm CO", "1150 ppm CO", "1500 ppm CO", "2050 ppm CO", "2400 ppm CO" and "2520 ppm CO". However, these fuel mixtures used differ not only in the CO content but also, proportionally, in the hydrogen concentration due to the dilution with He. The flow rate for both anode and cathode feed was kept at 170 cm^3/min in all the experiments.

The effect of varying the cell operating temperature and the partial pressure of H_2 in the fuel mixture was also investigated using the Pt/Nafion 117/Pt cell. As in the previous study [18], the saturators temperature was set at 80 °C. The cell was maintained in a vertical position in order to minimize the effect of H_2O flooding at the anode.

All the experiments were done galvanostatically using an AMEL 553 Galvanostat–Potentiostat. The analysis of the reaction products was carried out with an UNOR 6N IR CO analyzer and a PERKIN-ELMER SIGMA 300 HWD Gas Chromatograph utilising a Molecular Sieve column to separate CO, H_2 and N_2 and a Porapak N column to separate CO_2.

3. Results and discussion

3.1. Fuel cell operation

The first experiments were carried out in the normal fuel cell operation mode and using the Nafion 117 membrane, 2400 ppm CO mixture at the anode and air at the cathode, while monitoring the CO concentration at the exit of the anode compartment. Fig. 2 shows a transient obtained by varying the external resistive load and thus the cell current I. At the beginning, the circuit is open ($I = 0$) and the cell potential U is 0.72 V. The reason for this low emf is discussed below.

One first notices that even under open-circuit conditions there is a finite rate of consumption of CO, r^o_{CO} equal to 2.2×10^{-9} mol/s. This consumption of CO appears, at a first glance, to be entirely due to the water–gas-shift reaction (WGS):

$$CO + H_2O \rightarrow CO_2 + H_2 \quad (3)$$

Upon decreasing the external resistive load at $t = 0$, so that $I = 0.5$ mA, one observes, as expected, a decrease in the cell potential ($U = 0.4$ V) and an increase, Δr, in the rate of CO consumption. Upon opening the circuit, the potential, U, and the rate of CO consumption return to their initial values.

The increase in the rate of CO consumption, $\Delta r = 4.4 \times 10^{-9}$ mol/s, is a factor of 2 larger than the open-circuit catalytic rate of CO consumption ($\rho = 3$, Eq. (2)) and interestingly, a factor of 80% larger than that corresponding via Faraday's law to the rate of electrochemical CO oxidation $I/2F = 2.6 \times 10^{-9}$ mol/s. Thus, even if all the current corresponds to CO oxidation, i.e. to WGS and subsequent H_2 oxidation (and not at all to extra H_2 oxidation) the effect is non-Faradaic and one would reasonably conclude that this is due to the electrochemical promotion (NEMCA) of the WGS reaction (3).

This is further corroborated by examining systematically the effect of cell current, I, and rate of H_2 transport, $I/2F$, on the increase in consumption of CO (Fig. 3). One observes that over certain ranges of current values the Faradaic efficiency Λ exceeds unity. The effect is more pronounced when using thinner (1135) Nafion membranes [18].

The explanation is that O_2 (and thus, of course H_2) crossover through the membrane is significant and that this "crossover" O_2 reaching the anode is, at least partly, responsible for the open-circuit rate, r^o_{CO}, of CO consumption and second that the same crossover oxygen promotes the rate of the WGS reaction.

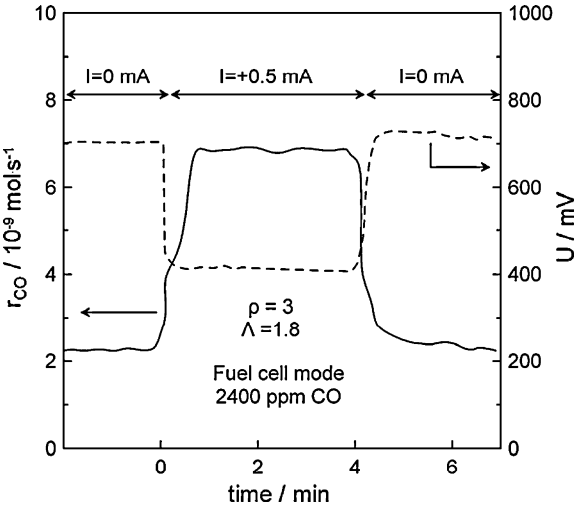

Fig. 2. CO consumption rate, r_{CO}, and cell potential response to step changes in the external resistance and thus in fuel cell current. The rate increase, Δr_{CO}, is 80% larger than the H_2 removal from the anode, $I/2F$ ($\Lambda = 1.8$). Anode fed with the "2400 ppm CO" reformate mixture, $T = 30$ °C.

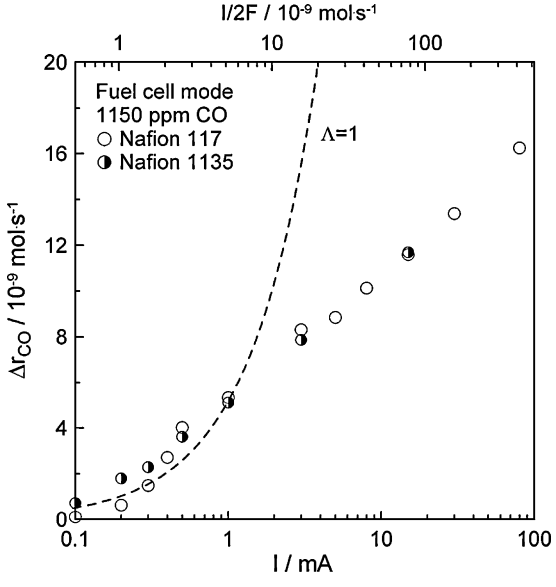

Fig. 3. Dependence of the change in CO consumption rate on the cell current during fuel cell operation with Pt electrodes and two Nafion membranes of different thickness. The anode is fed with "1150 ppm CO" reformate mixture. The unpromoted catalytic rate is $r_o = 1.31 \times 10^{-9}$ mol/s for the Pt/Nafion 1135/Pt cell and $r_o = 0.65 \times 10^{-9}$ mol/s for the Pt/Nafion 117/Pt cell. The $\Lambda = 1$ curve is shown for comparison, $T = 30$ °C.

In order to further investigate these points we have carried out experiments by maintaining the same anodic gas composition and replacing at the cathode the air stream by a 1% H_2 in He stream.

3.2. Experiments with H_2 at the cathode

We refer to these experiments as "H_2 pumping" experiments. The galvanostat was used to impose currents in the same direction as those corresponding to fuel cell operation, i.e. with protons flowing from the anode to the cathode.

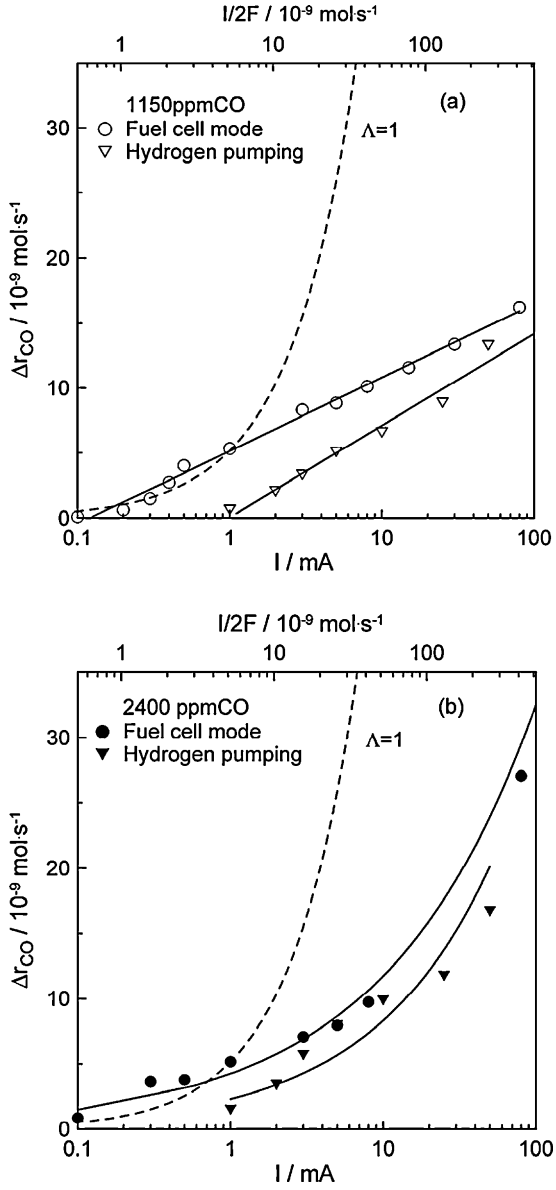

Fig. 4. Dependence of the change in CO consumption rate on the cell current during fuel cell operation (feeding air to the cathode) and hydrogen pumping operation (feeding 1% H_2/He to the cathode) with a Pt/Nafion117/Pt cell, showing the effect of the oxygen crossover, for anode feed gas composition of "1150 ppm CO" (a) and "2400 ppm CO" (b). The unpromoted catalytic rate r_o is 0.65×10^{-9} mol/s for fuel cell operation and 0.35×10^{-9} mol/s for hydrogen pumping operation at 1150 ppm CO, and 2.91×10^{-9} mol/s for fuel cell operation and 1.52×10^{-9} mol/s for hydrogen pumping operation at 2400 ppm CO. The $\Lambda = 1$ curve is shown for comparison, $T = 30$ °C.

Fig. 4 shows the effect of current, I, and rate of H_2 pumping, $I/2F$, on the increase in the rate of CO consumption, Δr_{CO}, and compares Δr_{CO} with that obtained in the normal fuel cell operation. The curve corresponding to $\Lambda = 1$, i.e. $\Delta r_{CO} = I/2F$, is also shown for comparison.

One observes two main features: First, the open-circuit catalytic rate, r^o_{CO}, is a factor of 2 larger in the case of fuel cell operation. This clearly shows that oxygen crossover is indeed taking place and that in fact, half of the CO consumed at the anode at open-circuit corresponds to the Pt catalyzed CO oxidation.

$$CO + \tfrac{1}{2}O_2 \rightarrow CO_2 \quad (4)$$

with remaining half corresponding to the WGS reaction (3).

Second, one observes that the Faradaic efficiency, Λ, is always smaller than that obtained in the normal fuel cell operation and, in fact, smaller than unity. These observations show conclusively that the crossover O_2 has a promoting effect on the WGS reaction so that in absence of O_2 the effect of current on the WGS reaction is sub-Faradaic ($\Lambda < 1$) while in presence of O_2 the effect of current and potential in reactions (3) and (4) becomes non-Faradaic ($\Lambda > 1$). Non-Faradaic electrochemical promotion of Pt and Pd catalysts in aqueous and Nafion environments have been already reported in the literature for H_2 oxidation [19,20] and *n*-butene isomerization [19–21].

In the present case, it is not easy to separate the effect of current on the NEMCA behavior of reactions (3) and (4). The use of isotopic $^{18}O_2$ at the cathode could elucidate this point. In any case, however, the present results show that a finite adsorbed oxygen coverage at the anode is necessary to induce electrochemical promotion on the Pt catalyst anode, in good agreement with the previous NEMCA studies of Pt in aqueous and Nafion environments [20,21].

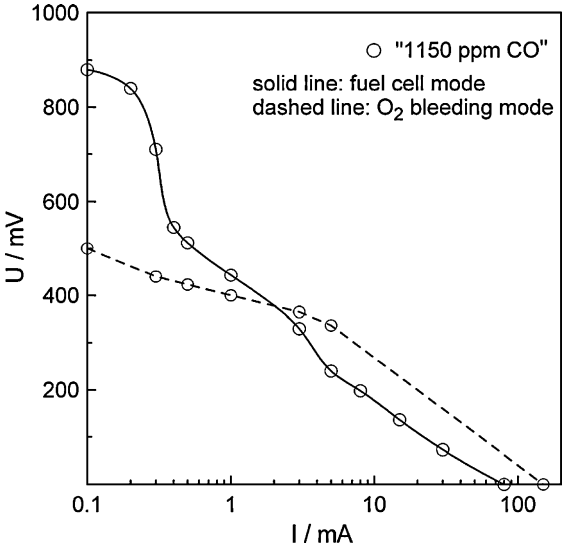

Fig. 5. Comparison of the cell current–potential performance in the fuel cell mode and O_2 bleeding mode. Anode fed with the "1150 ppm CO" reformate mixture, $T = 30$ °C.

3.3. O_2 bleeding experiments

In order to confirm the above points, a series of O_2 bleeding experiments was performed by admixing 1% O_2 with the anode gas. This leads, as expected, to a decrease in the open-circuit potential but, at the same time to an enhancement of the cell performance at higher current densities (Fig. 5). The thus obtained open-circuit catalytic rate of CO consumption, r^{o}_{CO}, was 7.2×10^{-9} mol/s versus 0.65×10^{-9} mol/s for normal fuel cell operation and 0.35×10^{-9} mol/s for the "H_2 pumping" mode. This clearly shows the effect of increasing p_{O_2} on the rate of CO oxidation, but also, as shown by the current-enhanced rate of CO oxidation (Fig. 6), on the electrochemical promotion of reactions (3) and (4), leading to Λ values up to 5.

Fig. 7 shows that O_2 bleeding enhances the Faradaic efficiency, Λ, but leads to smaller ρ values, i.e. up to 5 versus up to 25 for the case of normal fuel cell operation.

The temperature rise at the anode during the oxygen bleeding experiments was at most 2–3 K, which is too small to influence the cell performance to any significant extent.

3.4. Effect of temperature and p_{H_2}

As shown in Fig. 8, increasing the cell operating temperature to 80 °C, leads to enhanced overall cell performance, both for

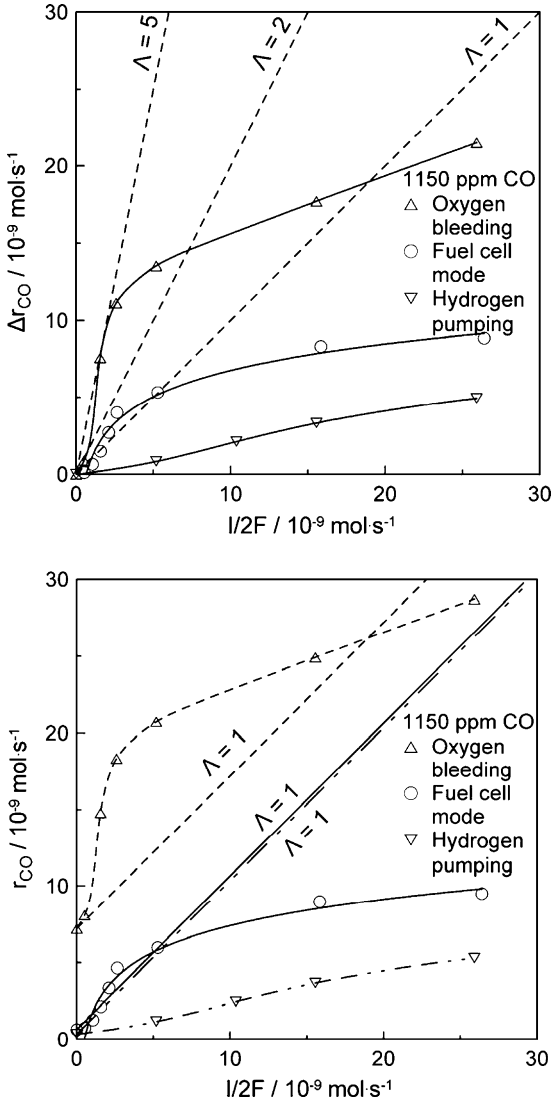

Fig. 6. Effect of current and concomitant, $I/2F$, rate of H_2 removal from the anode on the increase in the rate (top) and on the rate (bottom) of the CO consumption at the anode in the three different modes of operations of the Pt/Nafion 117/Pt cell. Dashed lines represent constant Λ values. The anode feed gas was the "1150 ppm CO" reformate mixture. The unpromoted catalytic rate r_o is 0.65×10^{-9} mol/s for fuel cell operation, 0.35×10^{-9} mol/s for hydrogen pumping operation and 7.20×10^{-9} mol/s for oxygen bleeding operation, $T = 30$ °C.

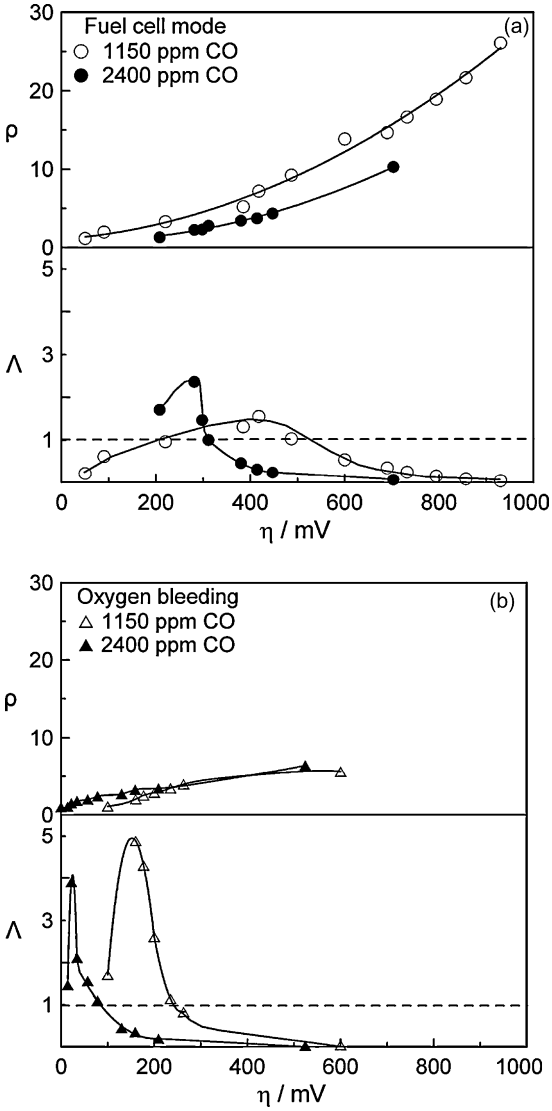

Fig. 7. (a) Rate enhancement ratio, ρ, and the Faradaic efficiency, Λ, dependence on the cell overpotential for fuel cell operation of a Pt/Nafion 117/Pt cell, for the two different anode feed gas compositions. The maximum ρ value is 26 and the maximum Λ value is 2.5. (b) Rate enhancement ratio, ρ, and the Faradaic efficiency, Λ, dependence on the cell overpotential during oxygen bleeding operation of the Pt/Nafion 117/Pt cell, for the two different anode feed gas compositions. The maximum Λ value is 5, $T = 30$ °C.

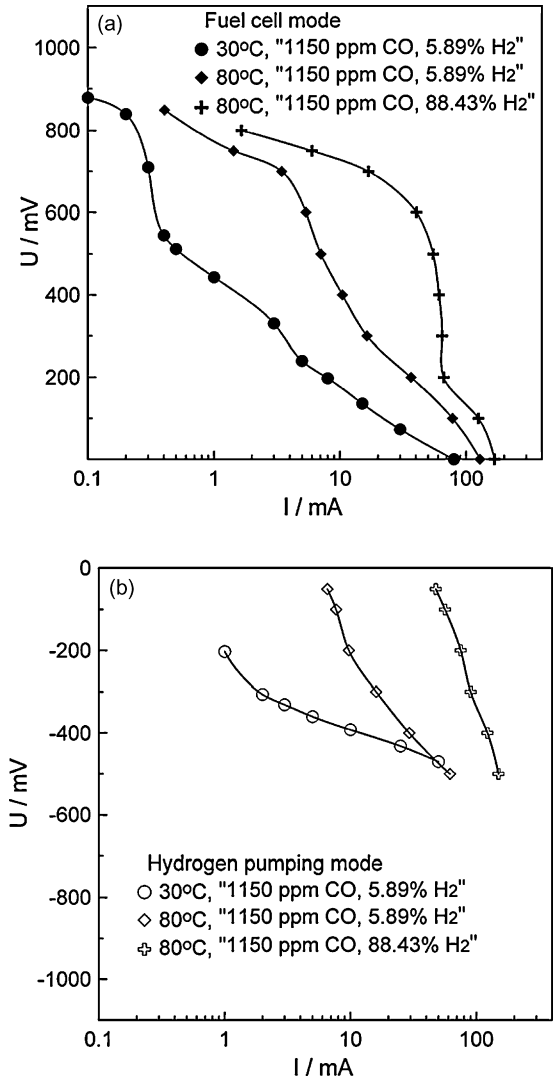

Fig. 8. Polarization *I–U* curves of a Pt/Nafion 117/Pt cell at different operation temperatures and the effect of increasing the partial pressure of H_2 in the fuel mixture during fuel cell operation (a) and hydrogen pumping operation (b). The anode feed gas was the ''1150 ppm CO'' reformate mixture.

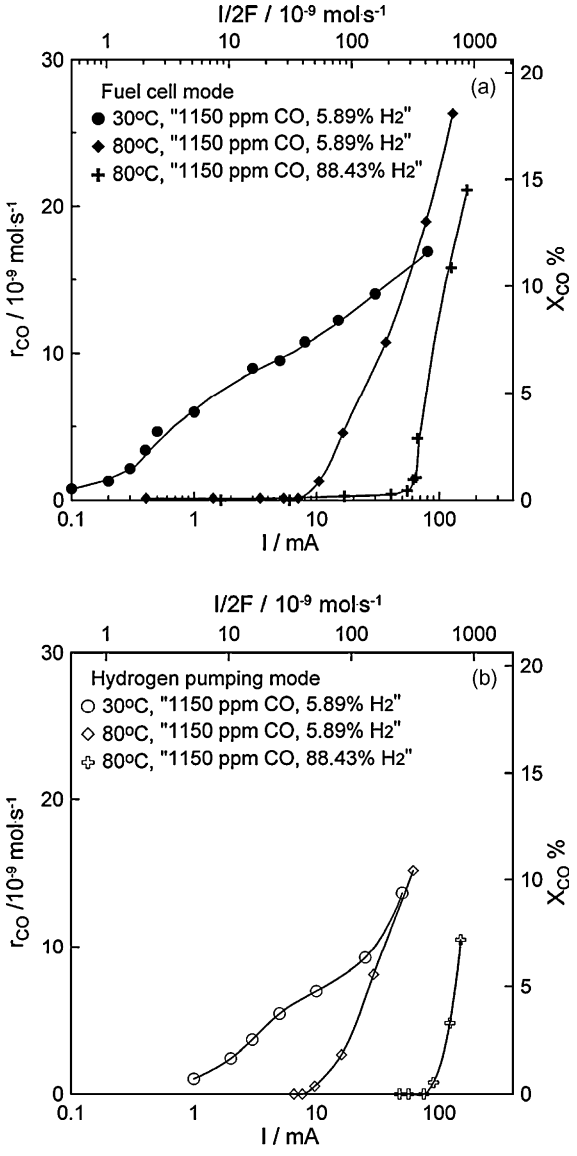

Fig. 9. Effect of current and concomitant, *I*/2*F*, rate of H_2 removal from the anode on the rate of the CO consumption at the anode in the fuel cell mode (a) and in the hydrogen pumping mode of operation (b) of the Pt/Nafion 117/Pt cell, at two operating temperatures and for different H_2 concentration in the fuel mixture. The anode feed gas was the ''1150 ppm CO'' reformate mixture.

the fuel cell and the hydrogen pumping operation. Moreover, as expected, increasing p_{H_2} further enhances significantly the cell performance.

Interestingly, increasing operating temperature leads to a decrease in CO conversion both in the fuel cell mode and in the hydrogen pumping mode, which is accompanied by a very significant increase in current (Fig. 9). This very likely indicates that under these higher temperature conditions, where CO adsorption is weaker, most of the surface sites of the Pt electrocatalyst are involved in H_2 oxidation with few sites remaining available for CO and also H_2O (or OH) adsorption and thus for the WGS reaction.

This competition between the two reactions (H_2 adsorption and oxidation and WGS reaction) is also manifested in Fig. 10, which shows that increasing H_2 concentration in the fuel mixture further suppresses the increase in CO consumption and the CO conversion Faradaic efficiency.

3.5. PtCu/C catalysts

When using the PtCu catalyst at the anode, the cell power output is lower than that obtained with the Pt anode. The currents obtained with the PtCu catalyst are of the order of μA. The Tafel plots obtained during both modes of the cell operation are shown in Fig. 11. At the same time the rate of CO consumption is significantly larger than on the Pt anode (Table 1 and Fig. 12).

The rate of CO consumption for open-circuit conditions and for two different values of the applied current is shown in Fig. 12 for the five fuel mixtures used, during fuel cell operation and hydrogen pumping operation. The same figure shows that the CO consumption rate increases with increasing positive

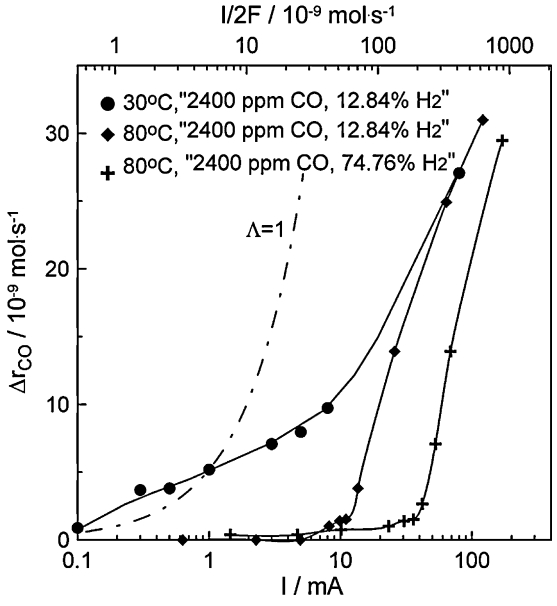

Fig. 10. Effect of current and concomitant, $I/2F$, rate of H_2 removal from the anode on the increase in the rate of the CO consumption at the anode during fuel cell operation of the Pt/Nafion 117/Pt cell, increasing the cell temperature and the hydrogen concentration in the fuel mixture. The dashed line represents constant Λ value equal to 1. The anode feed gas was the "2400 ppm CO" reformate mixture.

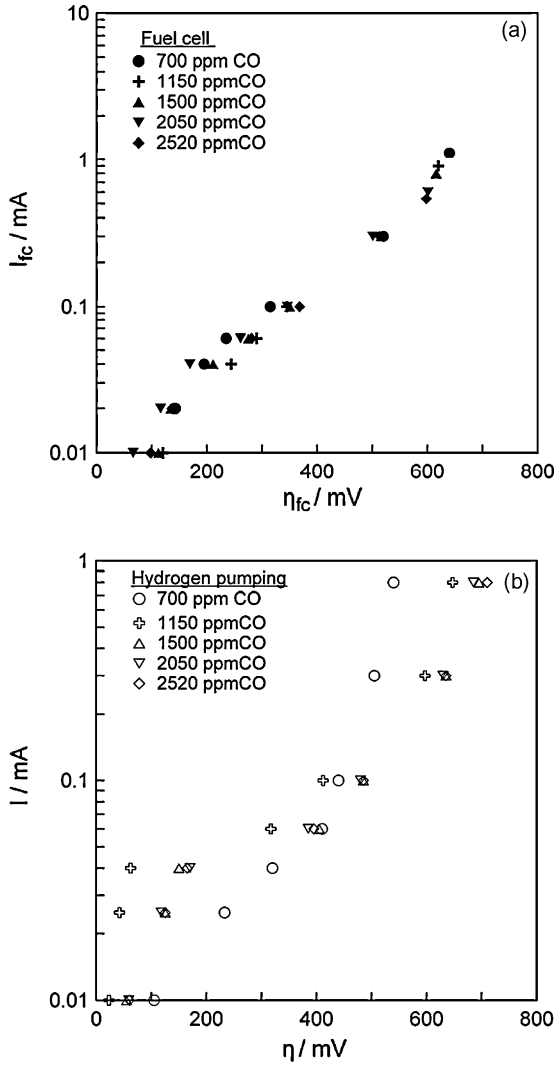

Fig. 11. Tafel plots for a PtCu/Nafion 117/Pt cell during fuel cell operation (a) and hydrogen pumping operation (b), for five different CO concentrated fuel mixtures, at 30 °C.

current. Also, due to oxygen crossover, the rates are generally larger in the case of fuel cell operation than during the hydrogen pumping operation.

Significant non-Faradaic behavior is observed when using the PtCu catalyst, and the values of the Faradaic efficiency Λ are much higher than those corresponding to the Pt catalyst. This is in qualitative agreement with the higher open-circuit rates of CO consumption on the PtCu anode and the approximate expression $\Lambda \approx 2Fr_o/I_o$ [13], which predicts higher Λ values for larger open-circuit rates. Thus, in the case of PtCu anode, non-Faradaic behavior observed both in the fuel cell operation and in the hydrogen pumping operation (Fig. 13). Comparing the maximum Λ values obtained during fuel cell operation and hydrogen pumping operation for different CO concentrations (Fig. 13), one observes that the non-Faradaic behavior is more pronounced in presence of oxygen (fuel cell operation), showing again the significant role of oxygen crossover.

In general, the measured Λ values are a factor of 10 smaller than those predicted by the approximate expression $2Fr_o/I_o$ [13], where I_o is the exchange current. This is due to the fact that the above theoretical equation is based [13] on the assumption that $\alpha = \alpha_a$ where α_a is the anodic transfer coefficient and α is the NEMCA coefficient [13], which is typically of the order 0.5–1. In the present case, however, as can be seen in Fig. 8, the measured α_a values are very small, typically, 0.2. Consequently [13], the expected Λ values are significantly smaller than $2Fr_o/I_o$, as experimentally observed.

Table 1
Comparison of PtCu and Pt anodes

p_{CO} (kPa)	r^o_{CO} Fuel cell mode ($\times 10^{-9}$ mol s^{-1})		r^o_{CO} H_2 pumping mode ($\times 10^{-9}$ mol s^{-1})	
	PtCu anode	Pt anode	PtCu anode	Pt anode
0.070	4.36		4.31	
0.115	5.65	0.65	4.61	0.35
0.150	7.74		7.29	
0.205	10.27		8.63	
0.252	13.54	2.91	10.27	1.52

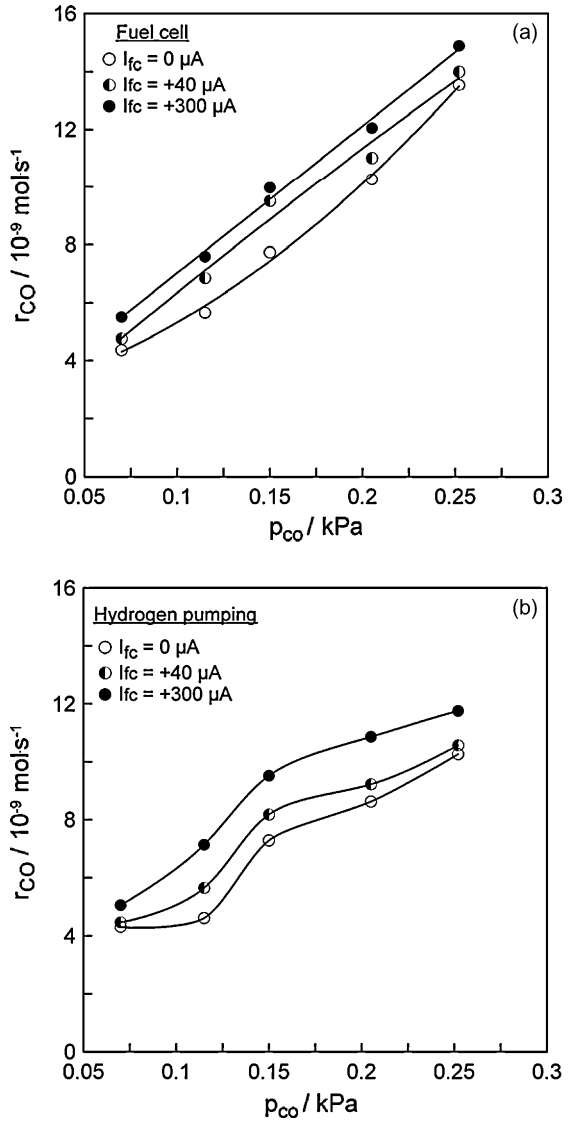

Fig. 12. Effect of partial pressure of CO in the fuel mixture on the rate of CO consumption for different values of the applied current, in presence of O_2 (fuel cell mode) (a) and in absence of O_2 (hydrogen pumping mode) (b) of operation of the PtCu/Nafion 117/Pt cell, at 30 °C.

Most previous electrochemical promotion studies using aqueous electrolytes [13,16] or Nafion [13] have shown Λ values typically of the order of 10 as in the present study. However, significantly larger Λ values have been measured in the case of 1-butene isomerization on Pd/Nafion [19], or in the case of ceramic proton conductors [13]. As shown in Fig. 7a and b the rate enhancement ratio, ρ, reaches values up to 30, while the Faradaic efficiency, Λ, exhibits a maximum at intermediate total overpotential, η_{FC}, value which moves to lower η_{FC} values upon increasing the partial pressure of CO. This is similar to the rate maximum of CO oxidation observed in heterogeneous catalysis [13] and in the electrochemical promotion of CO oxidation on Pt/β''–Al_2O_3 [13] and thus, since the Λ varies linearly with r_o [13], the Λ maximum may correspond, as in the previous cases, to equal coverages of CO and OH^- on the catalyst surface.

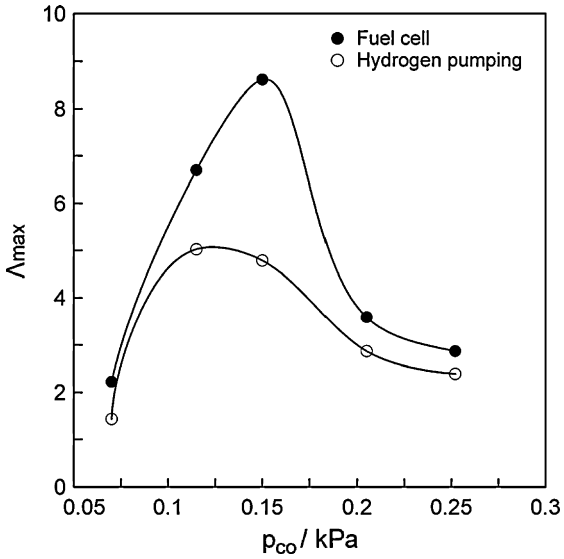

Fig. 13. Effect of partial pressure of CO in the fuel mixture on the maximum Λ value obtained in presence of O_2 (fuel cell mode) and in absence of O_2 (hydrogen pumping mode) during the operation of the PtCu/Nafion 117/Pt cell, at 30 °C.

4. Conclusions

The electrochemical promotion of the WGS reaction was studied in PEM fuel cells operating in three different modes (fuel cell operation, hydrogen pumping operation and oxygen bleeding operation). The results with Pt anodes provide strong evidence that the non-Faradaic behavior is mainly due to CO oxidation by oxygen which migrates via crossover through the Nafion membrane rather than to electropromotion of the water–gas-shift reaction itself. Electrochemical promotion was found in the normal fuel cell mode (Λ up to 2.5) and with oxygen bleeding operation (Λ up to 5), while sub-Faradaic behavior was observed in absence of oxygen in the reaction mixture (hydrogen pumping operation). Since oxygen crossover is responsible for the non-Faradaic consumption of CO via CO oxidation and the water–gas-shift reaction, higher Λ values are obtained with thinner Nafion membrane. It thus appears that O_2 crossover has a beneficial effect on the performance of CO-poisoned PEM fuel cells, due to the non-Faradaic enhancement in the rate of CO consumption at the anode. In the case of the PtCu anode catalysts, although the current densities are much smaller, the rate of CO consumption is comparable to that on Pt anodes and the Faradaic efficiency is much higher.

Acknowledgements

We thank Dr. S. Balomenou, Dr. D. Tsiplakides for helpful discussions, Professor E. Smotkin and his company, NuVant, for supplying us with the state-of-the-art PEMFC unit. We also thank DuPont (Drs. Simone Arizzi and Raj Rajendran) for supplying us with the Nafion membranes. Partial financial support from BASF and from the Hellenic General Secretariat of Research and Technology AKMON Programme is gratefully acknowledged.

References

[1] M. Wagner, N. Schulze, Electrochim. Acta 48 (2003) 3899.
[2] S.J. Lee, S. Mukerjee, E.A. Ticianelli, J. McBreen, Electrochim. Acta 44 (1999) 3283.
[3] S. Gottesfeld, J. Pafford, J. Electrochem. Soc. 135 (1988) 2651.
[4] A.H. Thomason, T.R. Lalk, A.J. Appleby, J. Power Sources 135 (2004) 204.
[5] L.P.L. Carrette, K.A. Friedrich, M. Huber, U. Stimming, Phys. Chem. 3 (2001) 320.
[6] J. Divisek, H.F. Oetjen, V. Peinecke, V.M. Schmidt, U. Stimming, Electrochim. Acta 43 (1998) 3811.
[7] C. He, H.R. Kunz, J.M. Fenton, J. Electrochem. Soc. 148 (2001) A1116.
[8] A. Katsaounis, S.P. Balomenou, D. Tsiplakides, M. Tsampas, C.G. Vayenas, Electrochim. Acta 50 (2005) 5132.
[9] M.N. Tsampas, A. Pikos, S. Brosda, A. Katsaounis, C.G. Vayenas, Electrochim. Acta 51 (2006) 2743.
[10] R. Liu, E.S. Smotkin, J. Electroanal. Chem. 535 (2002) 49.
[11] B. Gurau, E.S. Smotkin, J. Power Sources 112 (2002) 339.
[12] C.G. Vayenas, S. Bebelis, S. Ladas, Nature 343 (1990) 625.
[13] C.G. Vayenas, S. Bebelis, C. Pliangos, S. Brosda, D. Tsiplakides, Electrochemical Activation of Catalysis: Promotion, Electrochemical Promotion and Metal-Support Interactions, Kluwer Academic/Plenum Publishers, New York, 2001
[14] R.M. Lambert, F. Williams, A. Palermo, M.S. Tihkov, Top. Catal. 13 (2000) 91.
[15] J. Nicole, D. Tsiplakides, S. Wodiunig, C. Comninellis, J. Electrochem. Soc. 144 (1997) 1312.
[16] S. Neophytides, D. Tsiplakides, P. Stonehart, M. Jaksic, C.G. Vayenas, Nature 370 (1994) 292.
[17] C.G. Vayenas, S. Brosda, C. Pliangos, J. Catal. 216 (2003) 487.
[18] F. Sapountzi, M. Tsampas, C.G. Vayenas, Top. Catal. 44 (2007) 461.
[19] L. Ploense, M. Salazar, B. Gurau, E.S. Smotkin, Solid State Ionics 136/137 (2000) 713.
[20] D. Tsiplakides, S. Neophytides, O. Enea, M.M. Jaksic, C.G. Vayenas, J. Electrochem. Soc. 144 (6) (1997) 2072.
[21] L. Ploense, M. Salazar, B. Gurau, E.S. Smotkin, JACS 119 (1997) 11550.